Circulatory CNP Rescues Craniofacial Hypoplasia in Achondroplasia

S. Yamanaka[1], Kazumasa Nakao[1], N. Koyama[1], Y. Isobe[1], Y. Ueda[2], Y. Kanai[2], E. Kondo[2], T. Fujii[2], M. Miura[2], A. Yasoda[2], Kazuwa Nakao[3], and K. Bessho[1]

Abstract

Achondroplasia is the most common genetic form of human dwarfism, characterized by midfacial hypoplasia resulting in occlusal abnormality and foramen magnum stenosis, leading to serious neurologic complications and hydrocephalus. Currently, surgery is the only way to manage jaw deformity, neurologic complications, and hydrocephalus in patients with achondroplasia. We previously showed that C-type natriuretic peptide (CNP) is a potent stimulator of endochondral bone growth of long bones and vertebrae and is also a potent stimulator in the craniofacial region, which is crucial for midfacial skeletogenesis. In this study, we analyzed craniofacial morphology in a mouse model of achondroplasia, in which fibroblast growth factor receptor 3 (FGFR3) is specifically activated in cartilage (*Fgfr3^ach* mice), and investigated the mechanisms of jaw deformities caused by this mutation. Furthermore, we analyzed the effect of CNP on the maxillofacial area in these animals. *Fgfr3^ach* mice exhibited midfacial hypoplasia, especially in the sagittal direction, caused by impaired endochondral ossification in craniofacial cartilage and by premature closure of the spheno-occipital synchondrosis, an important growth center in craniomaxillofacial skeletogenesis. We crossed *Fgfr3^ach* mice with transgenic mice in which CNP is expressed in the liver under the control of the human serum amyloid-P component promoter, resulting in elevated levels of circulatory CNP (*Fgfr3^ach*/*SAP-Nppc-Tg* mice). In the progeny, midfacial hypoplasia in the sagittal direction observed in *Fgfr3^ach* mice was improved significantly by restoring the thickness of synchondrosis and promoting proliferation of chondrocytes in the craniofacial cartilage. In addition, the foramen magnum stenosis observed in *Fgfr3^ach* mice was significantly ameliorated in *Fgfr3^ach*/*SAP-Nppc-Tg* mice due to enhanced endochondral bone growth of the anterior intraoccipital synchondrosis. These results clearly demonstrate the therapeutic potential of CNP for treatment of midfacial hypoplasia and foramen magnum stenosis in achondroplasia.

Keywords: chondrocyte(s), maxillofacial surgery, craniofacial anomalies, craniofacial biology/genetics, growth factor(s), growth/development

Introduction

Mammalian skeletons are formed through intramembranous or endochondral ossification. Most of the skeletons form by endochondral ossification through a process involving a cartilage intermediate. A small number of skeletal elements are formed by intramembranous ossification, in which bones form directly from condensations of mesenchymal cells without a cartilage intermediate (de Crombrugghe et al. 2001). The craniofacial skeleton contains bones that develop through both processes. Bones in the face and cranial vault develop through intramembranous ossification, whereas the skull base and nasal septum are formed through endochondral ossification (Takigawa et al. 1984; Takano et al. 1987).

Achondroplasia is the most common genetic form of human dwarfism, with a prevalence of 1/26,000 live births (Bellus et al. 1995; Cohen 1997). It is associated with constitutively active mutations in the gene encoding fibroblast growth factor receptor 3 (FGFR3) (Shiang et al. 1994). Craniofacial features of achondroplasia include a short cranial base, prominent forehead, midfacial hypoplasia, low nasal bridge, narrow nasal passages, spinal stenosis, foramen magnum stenosis, and short tubular bones (Thomas 1978; Elwood et al. 2003). The developmental mechanisms of midfacial hypoplasia and foramen magnum stenosis in achondroplasia are related to FGFR3 and mitogen-activated protein kinase (MAPK) signaling in chondrocytes, which regulates synchondrosis closure, osteoblast differentiation, and bone formation (Matsushita et al. 2009). Midfacial hypoplasia typically causes occlusal abnormality. Foramen magnum stenosis can cause hydrocephalus, potentially resulting in brainstem compression, apnea, or sudden death (Arron et al. 2006).

[1]Department of Oral and Maxillofacial Surgery, Graduate School of Medicine, Kyoto University, Kyoto, Japan
[2]Department of Diabetes, Endocrinology and Nutrition, Graduate School of Medicine, Kyoto University, Kyoto, Japan
[3]TK Project, Medical Innovation Center, Kyoto University, Kyoto, Japan

A supplemental appendix to this article is available online.

Corresponding Author:
Kazumasa Nakao, Department of Oral and Maxillofacial Surgery, Graduate School of Medicine, Kyoto University, 54 Kawahara-cho, Shogoin, Sakyo-ku, Kyoto, 606-8507, Japan.
Email: knakao@kuhp.kyoto-u.ac.jp

Currently, surgery is the only option for clinical management of jaw deformity resulting from midfacial hypoplasia and foramen magnum stenosis (Bagley et al. 2006). We previously showed that C-type natriuretic peptide (CNP), a member of the natriuretic peptide family (Nakao et al. 1992), is a potent stimulator of endochondral ossification (Chusho et al. 2001) and is dependent on guanylyl cyclase-B (GC-B)–mediated intracellular cGMP production (Suga et al. 1992). Further, CNP and GC-B are both expressed in the growth plates of long bones and vertebrae, and mice lacking CNP or GC-B exhibit severely impaired growth of these bones (Chusho et al. 2001; Tamura et al. 2004). We recently demonstrated that the CNP/GC-B system in the growth plate stimulates the proliferation of chondrocytes in the proliferative chondrocyte layer (Nakao et al. 2015). By contrast, mice with elevated circulatory CNP or targeted overexpression of CNP in growth plate cartilage exhibit prominent skeletal overgrowth (Yasoda et al. 2004; Kake et al. 2009; Yasoda et al. 2009) and longitudinal overgrowth along the cranial length through endochondral ossification (Nakao et al. 2013; Nakao et al. 2016).

Based on these findings, we hypothesized that the CNP/GC-B system represents a novel therapeutic target for the treatment of craniofacial hypoplasia in achondroplasia. To test this idea, we studied the effect of CNP on craniofacial hypoplasia in achondroplasia, using a mouse model of achondroplasia in which FGFR3 is specifically activated in cartilage.

Materials and Methods

Animals

Mice were housed in the specific pathogen–free animal facility of the Graduate School of Medicine, Kyoto University, under a 12-h light/dark cycle with ad libitum access to standard rodent diet and tap water. Animal care and experiments were conducted in accordance with institutional guidelines.

Mice expressing activated FGFR3 in the cartilage ($Fgfr3^{ach}$ mice) were generated on a FVB/N background using the $Col2a1$ promoter and enhancer sequences, as previously described (Naski et al. 1998). Mice expressing mouse CNP in the liver under the control of the human serum amyloid-P (SAP)–component promoter (SAP-$Nppc$-Tg mice) were generated on a C57BL/B6 background as previously described. These mice have elevated circulating CNP levels, and plasma CNP concentrations measured by radioimmunoassay (RIA) were 84% higher in SAP-$Nppc$-Tg mice than in wild-type (WT) mice (Kake et al. 2009). $Fgfr3^{ach}$ and SAP-$Nppc$-Tg mice were crossed to generate $Fgfr3^{ach}$ mice with elevated circulatory CNP levels ($Fgfr3^{ach}$/SAP-$Nppc$-Tg mice). In this study, all achondroplastic mice were heterozygous for the $Fgfr3^{ach}$ transgene. We used female F1 mixed-background (C57BL/B6; FVB/N) mice (WT, $Fgfr3^{ach}$, and $Fgfr3^{ach}$/SAP-$Nppc$-Tg) in all experiments. The genetic background of the controls in the present study is different from the previous one (Naski et al. 1998). The study conformed to ARRIVE (Animal Research: Reporting of In Vivo Experiments) guidelines for preclinical studies.

Skull Imaging

Three-dimensional reconstructions were generated by micro–computed tomography (μCT, SMX-100CT-SV3; Shimadzu Co.). μCT data were analyzed according to linear measurements and Euclidean distance matrix analysis (EDMA, http://www.getahead.psu.edu/) as described previously (Richtsmeier et al. 2000; Arron et al. 2006; Nakao et al. 2013). In addition, soft x-ray analyses were performed using an SRO-M5 system (30 kVp, 5 mA for 1 min; Softron). The size of the foramen magnum was measured using the ImageJ software (National Institutes of Health).

Organ and Micromass Cultures

Cranial bases and nasal septal cartilage (NSC) were obtained from neonatal WT or $Fgfr3^{ach}$ mice. Organ cultures of cranial bases and occipital bones treated with vehicle or 10^{-7} M CNP for 6 d were used to measure the length of the spheno-occipital synchondrosis (SOS), intersphenoidal synchondrosis (ISS), and anterior intraoccipital synchondrosis (AIOS) using a dissecting microscope equipped with linear ocular scale (10×; MZFL-III; Leica Microsystems) (Lei et al. 2008; Nakao et al. 2013). Micromass chondrocytes from NSC were cultured with vehicle or 10^{-7} M CNP for 3 wk and subsequently fixed with 10% formalin, embedded in paraffin, cut into 5-μm sections, and stained with Alcian blue/hematoxylin and eosin (HE) (Nakao et al. 2013).

Histology

Five-micron sections were cut from paraffin-embedded horizontal sections of cranial base and subsequently deparaffinized, rehydrated, stained with Alcian blue, and counterstained with HE (Muto Pure Chemicals Co.) as previously described (Nakao et al. 2013).

Immunohistochemistry

Type I and type II collagen (1310-10 and 1320-01; SBA), type X collagen (LB-0092; LSL), and von Willebrand factor (A0082; DAKO) were detected in tissue sections using the appropriate monoclonal antibodies.

TUNEL and BrdU Analysis

Target skeletal tissues were harvested 2 h after intraperitoneal injection of 5-bromo-2′-deoxyuridine (BrdU; 10 mL/kg; Nacalai), fixed overnight in 4% paraformaldehyde, and subsequently decalcified in 0.5 M EDTA for 2 wk. Samples were then embedded in paraffin and sectioned to detect BrdU-positive cells using anti-BrdU antibody (11296736001; Roche). Proliferation index was defined as the number of BrdU-positive nuclei, expressed as a percentage of the total number of nuclei in the proliferation zone in the SOS.

Terminal deoxynucleotidyl transferase–mediated dUTP nick end labeling (TUNEL) was performed under light microscopy (S7100; Millipore).

Real-Time Reverse-Transcription Polymerase Chain Reaction

Total RNA was extracted using the RNeasy Mini Kit (Qiagen) from NSC-derived micromass chondrocytes treated with vehicle or 10^{-7} M CNP for 10 d. Reverse-transcription polymerase chain reaction (RT-PCR) was performed as previously described (Nakao et al. 2013). Real-time RT-PCR was performed in a StepOne real-time PCR System (Applied Biosystems).

Statistical Analysis

Data are expressed as means ± standard error of the mean (SEM). Statistical analysis was performed in Excel (Microsoft) by analysis of variance (ANOVA) using Fisher's least significant difference method, and *P* values <0.05 were considered statistically significant. A nonparametric statistical technique was used for EDMA.

Supplemental Information

Detailed materials and methods (manufacturer, experimental condition, tables of the number of mice, etc.) are in the online Appendix.

Results

Morphologic Analyses of Skulls of WT, Fgfr3^ach, and Fgfr3^ach/SAP-Nppc-Tg Mice

Fgfr3^ach mice exhibited dwarfism and short limb bones (Fig. 1A, B). Skulls of *Fgfr3^ach* mice were longitudinally shorter than those of WT mice, as observed in skeletal preparations (Fig. 1C). μCT images were used for morphometric analyses of skulls from *Fgfr3^ach* mice (Fig. 1D). Nasal bone, upper jaw, and skull lengths in *Fgfr3^ach* mice were significantly shorter than those of WT mice (Fig. 1E). However, skull widths and inner-canthal distances were significantly larger in *Fgfr3^ach* than in WT crania (Fig. 1E). EDMA confirmed that nasal, premaxilla, maxilla, and frontal bones were markedly affected sagittally, resulting in hypoplasia in *Fgfr3^ach* crania (Fig. 1F). Conversely, cranial width was larger in *Fgfr3^ach* than in WT crania (Fig. 1F). μCT imaging revealed that both occipital and sphenoid bones that make the skull base were shorter in *Fgfr3^ach* than in WT mice (Fig. 1G, H). To study the effects of circulatory CNP on midfacial hypoplasia in *Fgfr3^ach* mice, we generated *Fgfr3^ach* mice with increased circulatory CNP levels by cross-mating *Fgfr3^ach* and *SAP-Nppc-Tg* mice. The resultant progeny (*Fgfr3^ach/SAP-Nppc-Tg* mice) exhibited attenuation of the *Fgfr3^ach* skeletal phenotype (Fig. 1A, B), consistent with our earlier report (Yasoda et al. 2009). Furthermore, hypoplasia of the skulls observed in *Fgfr3^ach* mice was markedly

attenuated in *Fgfr3^ach/SAP-Nppc-Tg* mice (Fig. 1C, D). Linear measurements obtained from μCT images revealed significantly improved skull length and nasal bone length in *Fgfr3^ach/SAP-Nppc-Tg* mice (Fig. 1E). EDMA revealed that the hypoplasia observed in *Fgfr3^ach* skulls was partially attenuated in *Fgfr3^ach/SAP-Nppc-Tg* skulls (Fig. 1F). Furthermore, the sphenoid bones were significantly improved and the occipital bones were partially improved in *Fgfr3^ach/SAP-Nppc-Tg* mice (Fig. 1G, H).

### Histological Analyses of SOS in WT, Fgfr3^ach, and Fgfr3^ach/SAP-Nppc-Tg Mice

Because endochondral ossification of the SOS determines the length of the skull base, the SOS is an important growth center in craniomaxillofacial skeletogenesis. We investigated the role of FGFR3 and determined the effect of CNP in synchondrosis closure using Alizarin red and Alcian blue staining of skull base preparations and Alcian blue/HE-stained horizontal sections in 10-d-old WT, *Fgfr3^ach*, and *Fgfr3^ach/SAP-Nppc-Tg* mice. In comparison with WT mice, skull bases of *Fgfr3^ach* mice exhibited 16.5% thinner SOS with ossification at the center of the SOS (Fig. 2A, B). Although the thickness of the SOS was significantly larger in *Fgfr3^ach/SAP-Nppc-Tg* than in *Fgfr3^ach* mice (Fig. 2C), SOS ossification was observed in *Fgfr3^ach/SAP-Nppc-Tg* but not in WT mice (Fig. 2B). Premature synchondrosis ossification was observed in 64% of *Fgfr3^ach* and 71% of *Fgfr3^ach/SAP-Nppc-Tg* mice at 1 wk old.

Immunostaining for type I collagen (marker of ossification) confirmed that synchondrosis ossification occurred at the center of SOS (Fig. 2D) in *Fgfr3^ach* skull base. In addition, staining of type II (marker for nonhypertrophic chondrocyte layer; Fig. 2E) and type X collagens (marker of hypertrophic chondrocyte differentiation; Fig. 2F) revealed that both nonhypertrophic and hypertrophic chondrocyte layers were reduced.

Synchondrosis ossification also occurred at the center of the SOS in the *Fgfr3^ach/SAP-Nppc-Tg* skull base (Fig. 2D), whereas both the nonhypertrophic and hypertrophic chondrocyte layers were thicker in *Fgfr3^ach/SAP-Nppc-Tg* than in *Fgfr3^ach* mice and comparable to those in WT mice (Fig. 2E, F).

Cells positive for von Willebrand factor, a marker of vascular endothelia, and for TUNEL, a marker of apoptosis, were clearly identifiable at the center (Fig. 2G) and edges (Fig. 2H), respectively, of the type I collagen–positive area of the SOS in *Fgfr3^ach* and *Fgfr3^ach/SAP-Nppc-Tg* mice.

We also examined the proliferation of chondrocytes in this region by staining for incorporated BrdU. BrdU-positive cells were clearly detected in the center of the type I collagen–positive area of the SOS in *Fgfr3^ach* and *Fgfr3^ach/SAP-Nppc-Tg* mice and in the proliferative zone in WT, *Fgfr3^ach*, and *Fgfr3^ach/SAP-Nppc-Tg* mice. The proportions of BrdU-positive chondrocytes were significantly lower in the proliferating layer of synchondroses in *Fgfr3^ach* than in WT mice (Fig. 2I). The proportions of BrdU-positive chondrocytes were clearly higher in *Fgfr3^ach/SAP-Nppc-Tg* than in *Fgfr3^ach* mice (Fig. 2I, J).
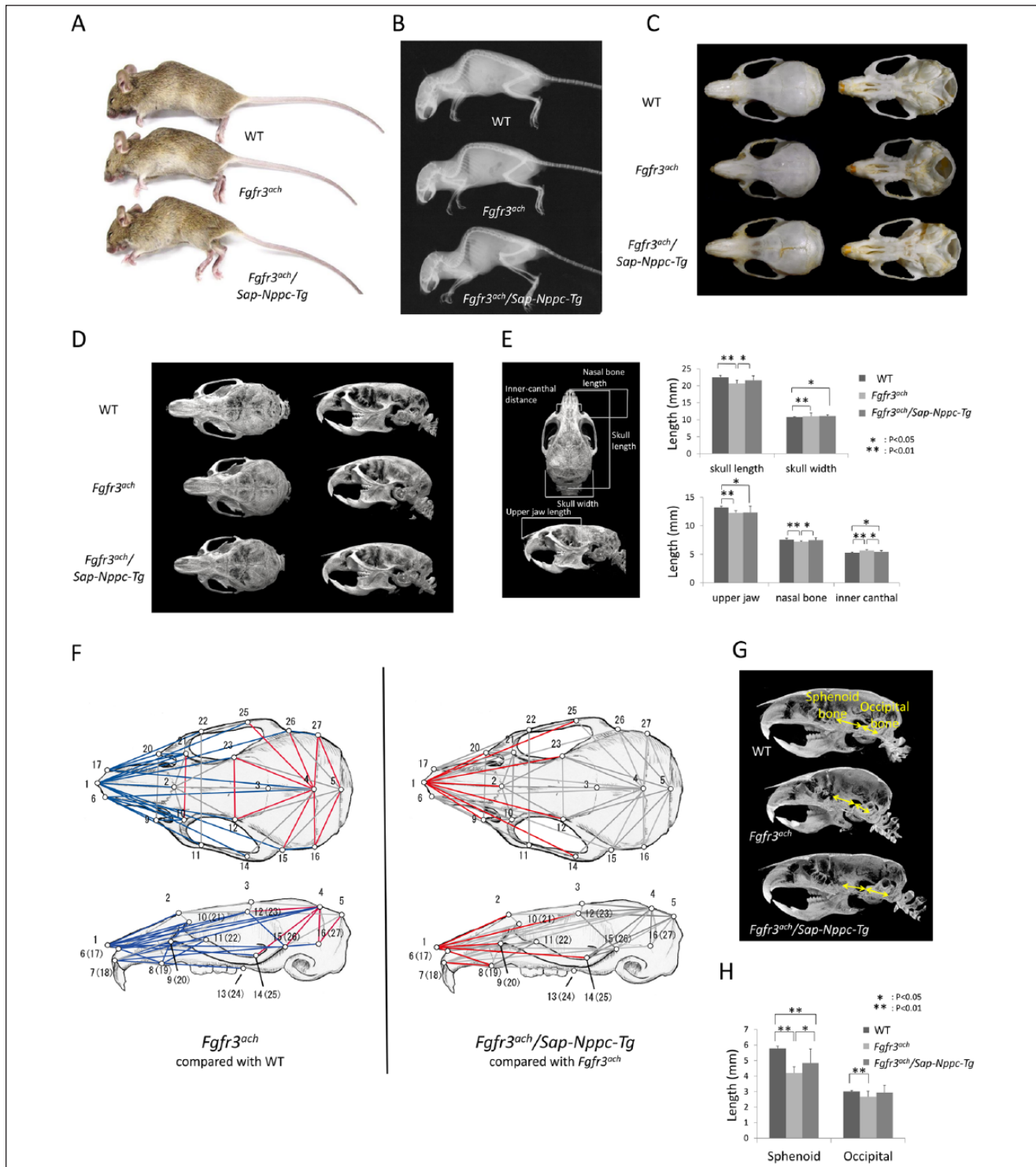
Figure 1. Craniofacial morphology of wild-type (WT), *Fgfr3^ach^*, and *Fgfr3^ach^/SAP-Nppc-Tg* mice. (**A**) Gross morphologies of 12-wk-old WT, *Fgfr3^ach^*, and *Fgfr3^ach^/SAP-Nppc-Tg* mice. (**B**) Soft x-ray picture from 12-wk-old WT, *Fgfr3^ach^*, and *Fgfr3^ach^/SAP-Nppc-Tg* mice. (**C**) Skeletal preparations from 12-wk-old WT, *Fgfr3^ach^*, and *Fgfr3^ach^/SAP-Nppc-Tg* mice. (**D**) Three-dimensional reconstructed images of the skulls of 12-wk-old WT, *Fgfr3^ach^*, and *Fgfr3^ach^/SAP-Nppc-Tg* mice. (**E**) Linear measurements for analysis of normal mouse skulls (left pictures). Linear measurements from 12-wk-old WT and *Fgfr3^ach^* mice (*n* = 12 each, *P* < 0.05 or 0.01) (right graph). (**F**) Landmarks used for Euclidean distance matrix analysis (EDMA). Schematic images of the mouse cranium (upper, superior view; lower, lateral view). Significantly smaller or larger values (*n* = 8, *P* < 0.05) are denoted by lines of different colors. Blue lines indicate significant hypoplasia, and red lines indicate significant hyperplasia. Gray lines indicate no significant difference. *Fgfr3^ach^* compared with WT mice (images at left) and *Fgfr3^ach^/Sap-Nppc-Tg* compared with *Fgfr3^ach^* mice (images at right). (**G**) Sagittal sections from micro–computed tomography (μCT) images of 12-wk-old WT, *Fgfr3^ach^*, and *Fgfr3^ach^/SAP-Nppc-Tg* mice. (**H**) Sagittal lengths of occipital and sphenoid bones from 12-wk-old WT, *Fgfr3^ach^*, and *Fgfr3^ach^/SAP-Nppc-Tg* mice (*n* = 12 each, *P* < 0.05 or 0.01).
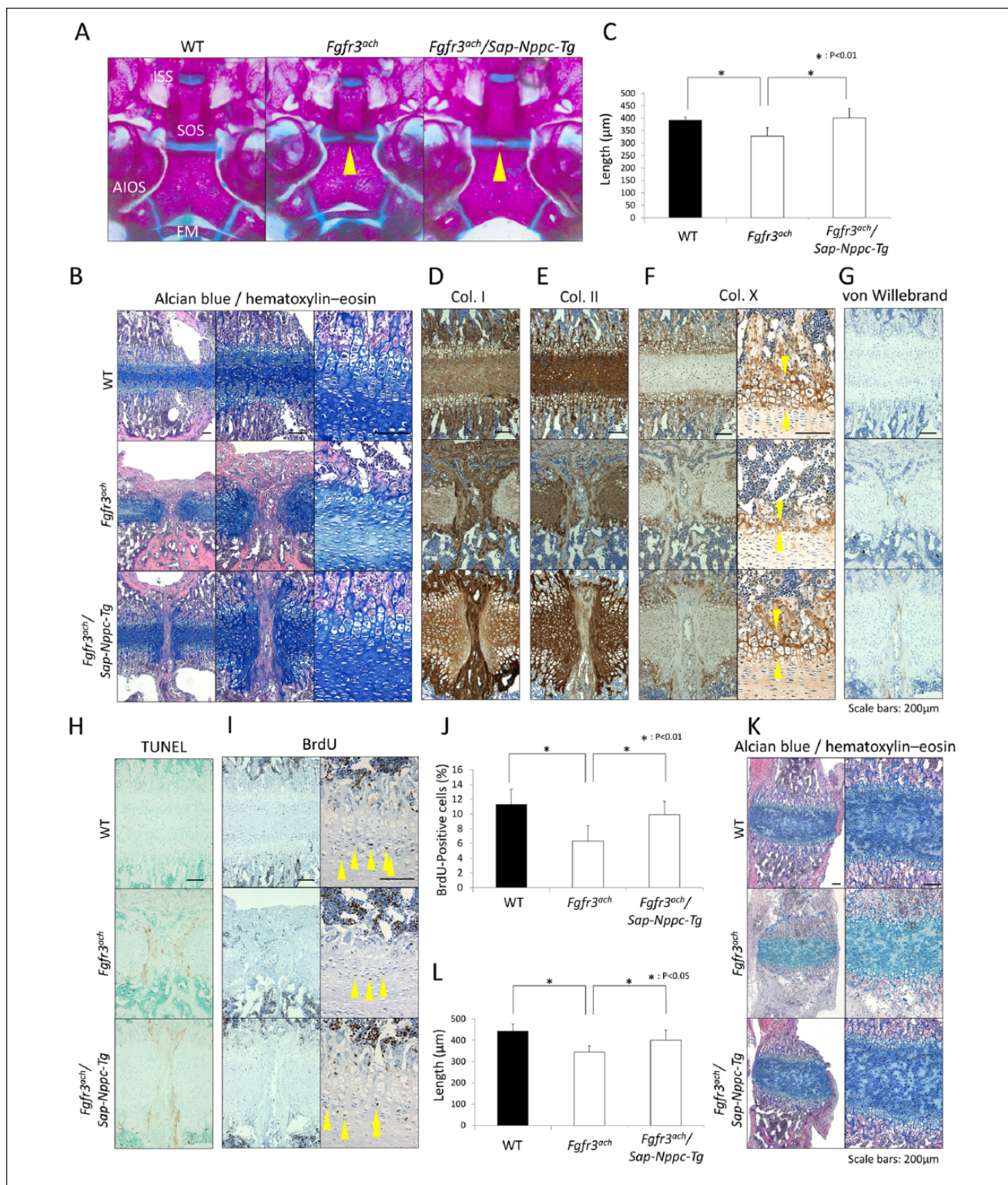
Figure 2. Histological analyses of spheno-occipital synchondrosis (SOS) and intersphenoidal synchondrosis (ISS) in wild-type (WT), *Fgfr3^ach^*, and *Fgfr3^ach^/SAP-Nppc-Tg* mice. (**A**) Alizarin red and Alcian blue staining of skull bases in 10-d-old WT and *Fgfr3^ach^* mice. Arrowhead indicates closure of the synchondrosis. Arrowheads indicate ossification of the SOS. (**B**) Alcian blue/hematoxylin and eosin (HE) staining in horizontal sections of the SOS of 10-d-old WT, *Fgfr3^ach^*, and *Fgfr3^ach^/SAP-Nppc-Tg* mice. (**C**) Histological lengths of SOS of WT, *Fgfr3^ach^*, and *Fgfr3^ach^/SAP-Nppc-Tg* mice ($n = 6$ each, $P < 0.01$). (**D–H**) Immunohistochemical analyses of type I collagen (D), type II collagen (E), type X collagen (F), von Willebrand factor (G), and terminal deoxynucleotidyl transferase–mediated dUTP nick end labeling (TUNEL) (**H**) in horizontal sections of the SOS of WT, *Fgfr3^ach^*, and *Fgfr3^ach^/SAP-Nppc-Tg* mice. Between arrowheads in F indicate hypertrophic chondrocyte layers. (**I**) Immunohistochemical staining for 5-bromo-2′-deoxyuridine (BrdU) of SOS from 10-d-old WT, *Fgfr3^ach^*, and *Fgfr3^ach^/SAP-Nppc-Tg* mice. The arrowheads indicate BrdU-positive cells. (**J**) The proliferative rate of chondrocytes in growth plate, shown as the average percentage of BrdU-positive cells ($n = 8$ each, $P < 0.01$). (**K**) Alcian blue/HE staining in horizontal sections of the ISS of 10-d-old WT, *Fgfr3^ach^*, and *Fgfr3^ach^/SAP-Nppc-Tg* mice. (**L**) Histological lengths of ISS of WT, *Fgfr3^ach^*, and *Fgfr3^ach^/SAP-Nppc-Tg* mice ($n = 6$ each, $P < 0.05$).
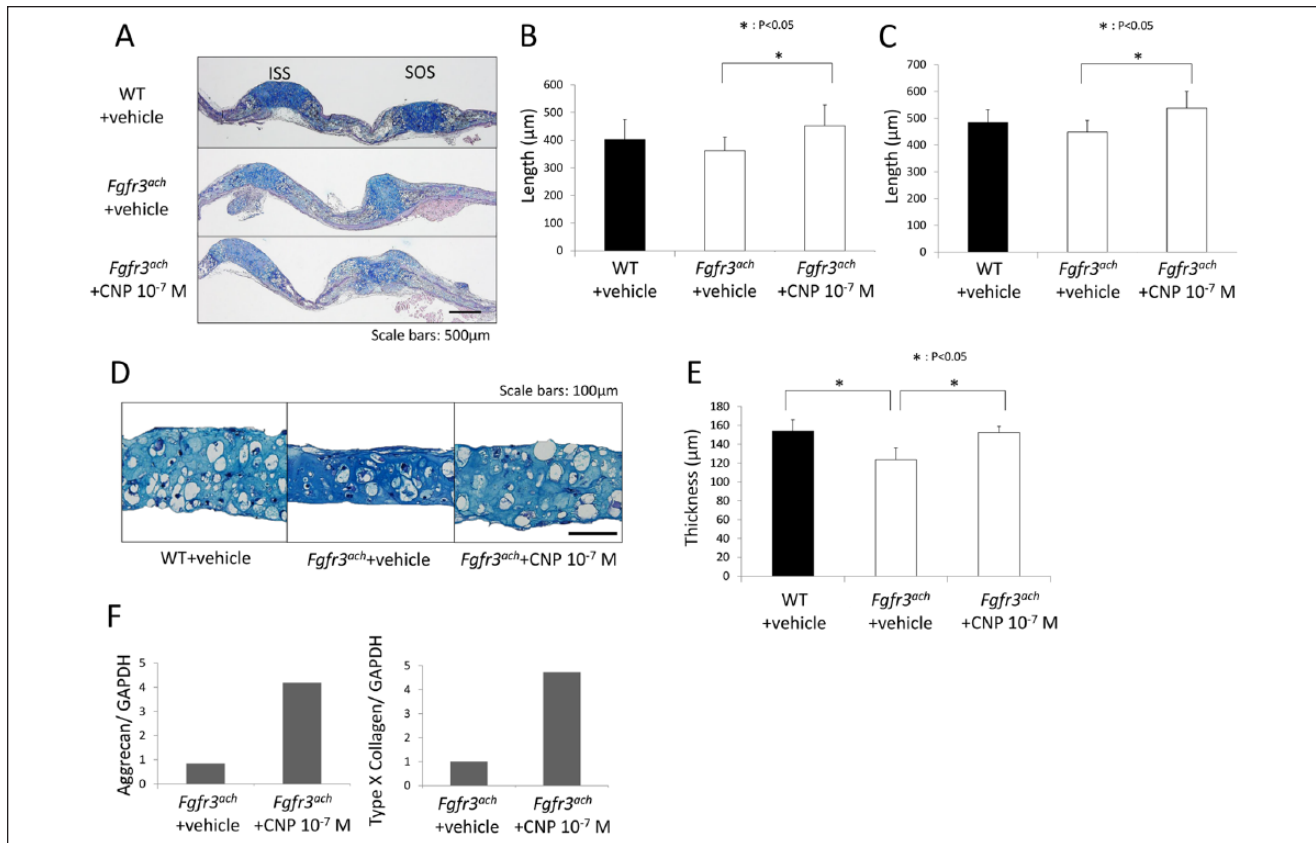
Figure 3. Mechanism of C-type natriuretic peptide's (CNP's) effect on impaired craniofacial skeletogenesis in *Fgfr3*^{ach} mice. (**A**) Histological examination of skull base after a 6-d organ culture and staining with Alcian blue/hematoxylin and eosin (HE) in skull base explants from neonatal wild-type (WT) and *Fgfr3*^{ach} mice treated with vehicle or 10^{-7} M CNP. (**B**, **C**) Histological lengths of intersphenoidal synchondrosis (ISS) (B) and spheno-occipital synchondrosis (SOS) (C) from organ-cultured WT and *Fgfr3*^{ach} mice treated with vehicle or 10^{-7} M CNP ($n = 10$ each, $P < 0.05$). (**D**) Histologic appearance of micromass cultures of nasal septal cartilage (NSC) from neonatal WT and *Fgfr3*^{ach} mice treated with vehicle or 10^{-7} M CNP. (**E**) Histological thickness of micromasses of WT and *Fgfr3*^{ach} mice treated with vehicle or 10^{-7} M CNP ($n = 5$ each, $P < 0.05$). (**F**) Expression of genes for aggrecan (left) and type X collagen (right) in NSC-derived micromass cultures from *Fgfr3*^{ach} mice treated with vehicle or 10^{-7} M CNP for 10 d, as determined by real-time reverse-transcription polymerase chain reaction (RT-PCR).

Histological Analyses of ISS in WT, Fgfr3^{ach}, and Fgfr3^{ach}/SAP-Nppc-Tg Mice

The ISS, a synchondrosis of the skull base, also contributes to the cranial base length, specifically of the sphenoid bone. The Alcian blue/HE-stained horizontal sections of the ISS revealed that the ISS was significantly 22.1% thinner in *Fgfr3*^{ach} than in WT mice. The narrowing of the ISS observed in *Fgfr3*^{ach} mice was also rescued in *Fgfr3*^{ach}/*SAP-Nppc-Tg* mice, as in the SOS. Furthermore, we observed premature ossification from the edge of the ISS in some *Fgfr3*^{ach} and *Fgfr3*^{ach}/*SAP-Nppc-Tg* mice but not in WT mice (Fig. 2K, L).

Organ Culture Experiments of Skull Base from WT and Fgfr3^{ach} Mice

To elucidate the effects of activated FGFR3 on the growth of ISS and SOS, as well as the effects of CNP on the growth of the ISS and SOS in *Fgfr3*^{ach} mice, we performed organ culture experiments using skull base explants from neonatal *Fgfr3*^{ach} and WT mice (Fig. 3A). At the end of a 6-d culture period, the ISS and SOS of skull base explants from *Fgfr3*^{ach} mice were approximately 9.6% and 3.3% shorter than those of WT explants, respectively (Fig. 3B, C). Treatment of *Fgfr3*^{ach} skull base with CNP significantly increased the lengths of the ISS and SOS (Fig. 3A–C).

Micromass Culture of NSC from WT and Fgfr3^{ach} Mice

Because the growth of the NSC is essential for longitudinal facial growth (Wealthall and Herring 2006), we examined the growth of chondrocytes from NSC of WT and *Fgfr3*^{ach} mice in micromass culture. Histological evaluation revealed that the micromass was significantly 9.7% thinner in *Fgfr3*^{ach} than in WT. CNP significantly increased the thickness of micromass chondrocytes from *Fgfr3*^{ach} NSC (Fig. 3D, E). Furthermore, CNP treatment resulted in enlarged chondrocytes and increased the extracellular space, as observed in Alcian blue–stained sections (Fig. 3D). Expression levels of chondrogenic differentiation markers in the micromass, particularly aggrecan, one of the major structural components of cartilage, and type X collagen were higher following CNP treatment (Fig. 3F).
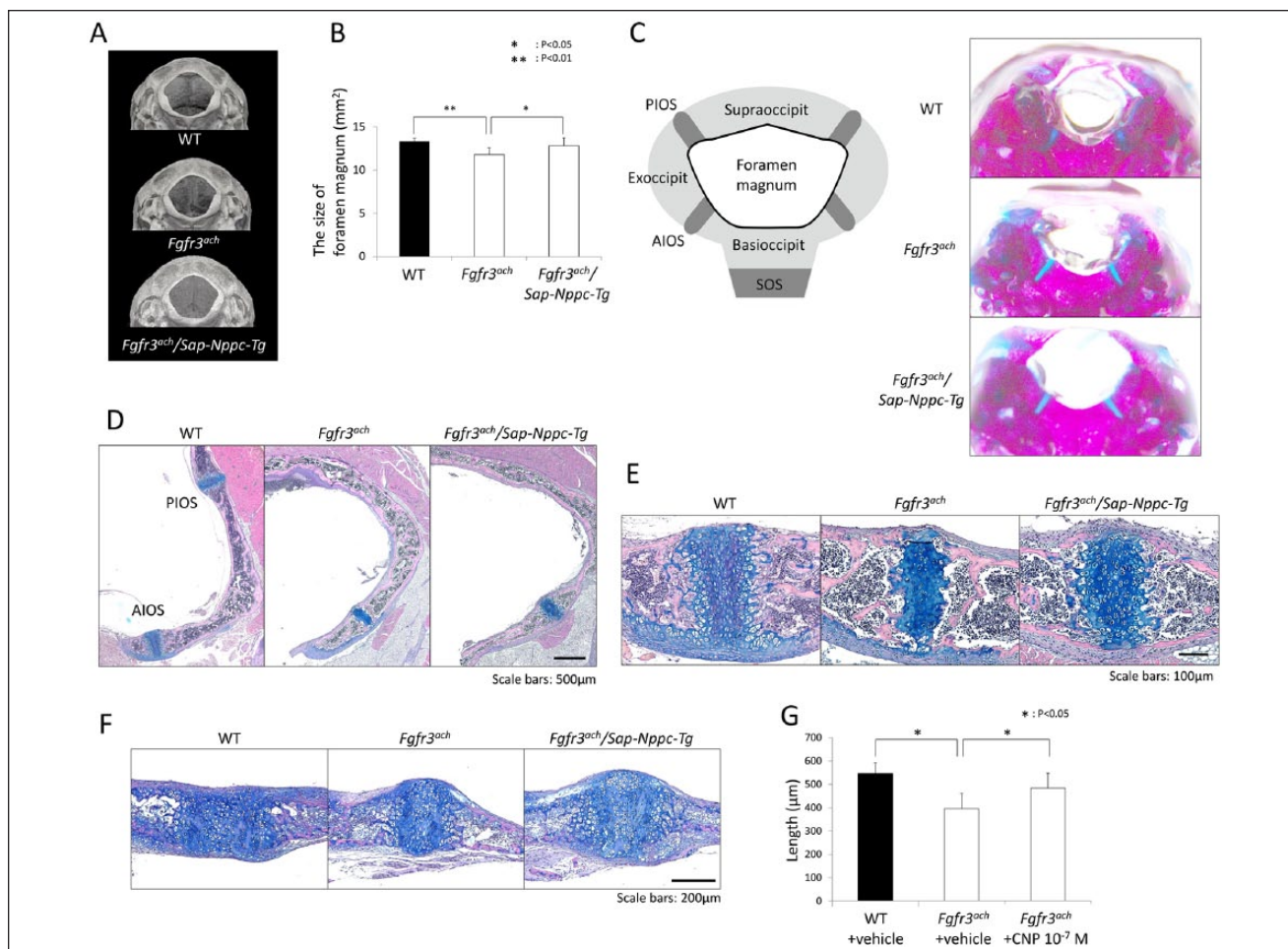
Figure 4. Mechanism of C-type natriuretic peptide's (CNP's) effect on foramen magnum stenosis in *Fgfr3*[ach] mice. (**A**) Three-dimensional reconstructed images of foramen magnum of 12-wk-old wild-type (WT), *Fgfr3*[ach], and *Fgfr3*[ach]/*SAP-Nppc-Tg* mice. (**B**) Sizes of foramen magnum of 12-wk-old WT, *Fgfr3*[ach], and *Fgfr3*[ach]/*SAP-Nppc-Tg* mice ($n = 8$ each, $P < 0.05$ or 0.01). (**C**) Illustration of the anatomy of the foramen magnum (image at left), and Alizarin red and Alcian blue staining of foramen magnum in 10-d-old WT and *Fgfr3*[ach] mice (images at right). (**D**) Alcian blue/hematoxylin and eosin (HE) staining in foramen magnum region of 10-d-old WT, *Fgfr3*[ach], and *Fgfr3*[ach]/*SAP-Nppc-Tg* mice. (**E**) Alcian blue/HE staining of anterior intraoccipital synchondrosis (AIOS) of WT, *Fgfr3*[ach], and *Fgfr3*[ach]/*SAP-Nppc-Tg* mice. (**F**) Histological examination of AIOS in occipital bone explants from neonatal WT and *Fgfr3*[ach] mice treated with vehicle or 10^{-7} M CNP for 6 d in organ culture, followed by staining with Alcian blue/HE. (**G**) Histological lengths of AIOS from organ-cultured WT and *Fgfr3*[ach] mice treated with vehicle or 10^{-7} M CNP ($n = 6$ each, $P < 0.05$).

Morphologic Analyses of Foramen Magnum of WT, Fgfr3[ach], and Fgfr3[ach]/SAP-Nppc-Tg Mice

To determine whether CNP is effective for treatment of foramen magnum stenosis caused by activation of FGFR3, we compared this region in WT, *Fgfr3*[ach], and *Fgfr3*[ach]/*SAP-Nppc-Tg* skulls (Fig. 4A). At 12 wk, the size of the foramen magnum was significantly smaller (–11.3%) in *Fgfr3*[ach] than in WT skulls. The narrowed foramen magnum of *Fgfr3*[ach] was rescued in *Fgfr3*[ach]/*SAP-Nppc-Tg* mice (Fig. 4B).

Histological Analysis of Foramen Magnum in WT, Fgfr3[ach], and Fgfr3[ach]/SAP-Nppc-Tg Mice

The foramen magnum is bound by the exoccipital, supraoccipital, and basooccipital bones, which develop and grow by endochondral ossification (Di Rocco et al. 2014). The AIOS

stands between the exoccipital and basooccipital bones, and the posterior intraoccipital synchondrosis (PIOS) stands between the exoccipital and supraoccipital bone (Fig. 4C). Staining of the AIOS with Alcian blue/HE revealed thinner synchondrosis in *Fgfr3*[ach] than in WT mice at 10 d old (Fig. 4D, E). Hypoplasia of the AIOS in *Fgfr3*[ach] mice was rescued by cross-mating with *SAP-Nppc-Tg* mice (Fig. 4E). On the other hand, although not observed in WT mice, synchondrosis ossification occurred at the PIOS in *Fgfr3*[ach] and *Fgfr3*[ach]/*SAP-Nppc-Tg* mice at 10 d old (Fig. 4C, D).

Organ Culture Experiments of Foramen Magnum from WT and Fgfr3[ach] Mice

To elucidate the effects of activated FGFR3 on the growth of the AIOS and the effects of CNP on AIOS growth in *Fgfr3*[ach] mice, we performed organ culture experiments using occipital

bones from neonatal *Fgfr3^ach^* and WT mice (Fig. 4F). At the end of a 6-d culture period, the AIOSs of occipital bones from *Fgfr3^ach^* mice were approximately 27.5% shorter than those in WT explants (Fig. 4G). Treatment with CNP during the culture period attenuated the hypoplasia of the AIOS in explants from *Fgfr3^ach^* mice (Fig. 4F, G).

Discussion

In this study, we analyzed the craniofacial morphology of *Fgfr3^ach^* mice and the mechanisms of jaw deformities caused by an achondroplasia-related mutation in FGFR3. *Fgfr3^ach^* mice exhibited maxillary hypoplasia similar to that of humans carrying the analogous mutation, as well as premature closure of the synchondrosis, consistent with previous reports (Matsushita et al. 2009). Furthermore, we found that premature synchondrosis closure initiates at the center of SOS in *Fgfr3^ach^* mice.

The premature synchondrosis closure was led by premature loss of proliferating chondrocytes, increased angiogenesis to the center of the SOS, and increased bone formation. Increased angiogenesis and bone formation further accelerated closure of the synchondrosis and fusion at ossification centers, and chondrocytes at the chondro-osseous junction of the SOS also underwent increased apoptosis. Histological assessment indicated reduced thickness of the hypertrophic and nonhypertrophic chondrocyte layers at the SOS and ISS in *Fgfr3^ach^* mice. Furthermore, in vitro organ and micromass culture studies suggested that FGFR3 signaling inhibited endochondral bone growth in the skull base and nasal septum. Consequently, *Fgfr3^ach^* mice crania exhibited hypoplasia in the sagittal direction, probably due to premature closure of the synchondrosis and impaired endochondral ossification. On the other hand, the elevated cranial width in *Fgfr3^ach^* mice could be attributed to increase intracranial pressure prior to fusion of the skull. This symptom is similar to the macrocephaly depending on hydrocephalus, observed in children with achondroplasia (Erdinçler et al. 1997).

In this experiment, foramen magnum stenosis, another typical feature also observed in achondroplasia patients, occurred in *Fgfr3^ach^* mice, and histological analysis revealed ossification of the PIOS and thinner AIOS in 10-d-old *Fgfr3^ach^* mice. Based on these results, we concluded that the foramen magnum stenosis in *Fgfr3^ach^* mice was caused by premature closure and impaired endochondral bone growth of the synchondroses of the foramen magnum, as in the synchondroses of the skull base.

Our earlier studies indicated that both systemic administration and targeted overexpression of CNP in cartilage attenuate impaired skeletal growth in the limbs and vertebrae of *Fgfr3^ach^* mice (Yasoda et al. 2004). Treatments with a CNP analogue also significantly restored bone growth in another mouse model of achondroplasia (Lorget et al. 2012). In addition to treating short stature, we hypothesized that the strong stimulatory effect of CNP on endochondral ossification could be useful in treating midfacial hypoplasia and foramen magnum stenosis in achondroplasia. To test this idea, we generated *Fgfr3^ach^/SAP-Nppc-Tg* mice with elevated plasma CNP concentrations (Kake et al. 2009). The choice to use a liver

targeted rather than a cartilage targeted CNP overexpressing mice is because it mimics intravascular administration of CNP. Consistent with this, *Fgfr3^ach^/SAP-Nppc-Tg* mice exhibited attenuated midfacial hypoplasia, possibly due to restoration of the thickness of the synchondrosis and promotion of the proliferation of chondrocytes in the craniofacial cartilage. The hypertrophic chondrocyte layers showed the most noticeable improvement. By promoting endochondral bone growth of the AIOS, *Fgfr3^ach^/SAP-Nppc-Tg* mice exhibited attenuated foramen magnum stenosis. Furthermore, in organ culture experiments using the skull base and occipital bone, as well as micromass cultures with NSCs, CNP increased matrix production and promoted the growth of hypertrophic chondrocytes in craniofacial cartilage of *Fgfr3^ach^* mice. Together, these results suggest that CNP may be useful in treating achondroplasia-related skull deformities.

We previously showed that CNP reverses the effects of FGFR3 signaling, which suppresses the proliferation and differentiation of growth plate chondrocytes and ultimately endochondral bone growth by inhibiting the MAPK pathway in tibiae (Yasoda et al. 2004). Because FGFR3 signaling promotes closure of the synchondrosis and fusion of ossification centers through the MAPK pathway (Matsushita et al. 2009), we hypothesized that the stimulatory effect of CNP also inhibits these processes. However, CNP did not suppress premature ossification of the SOS or PIOS in *Fgfr3^ach^/SAP-Nppc-Tg* mice. This lack of effect could be explained in 2 ways. First, early expression of CNP may be critical, and CNP expression in *SAP-Nppc-Tg* mice (which only occurs postnatally in this model) may have been too late (Zhao et al. 1992). Second, the circulating CNP concentration may have been too low to suppress ossification. These results indicate that early administration of CNP or a CNP analogue may be an important determinant of clinical effectiveness.

In summary, maxillary hypoplasia and foramen magnum stenosis caused by premature closure of the synchondrosis and impaired endochondral ossification in *Fgfr3^ach^* mice could be partially rescued by overexpression of CNP, thereby promoting endochondral ossification of craniofacial cartilage. CNP might be an effective therapy for the impaired skeletogenesis in the craniofacial region, including midfacial hypoplasia and narrowing of the foramen magnum, observed in patients with achondroplasia. Because administration of CNP or a CNP analogue is required before premature closure of the synchondrosis, early administration may be an important determinant of clinical effectiveness.

Author Contributions

S. Yamanaka, Kazumasa Nakao, A. Yasoda, contributed to conception, design, data acquisition, analysis, and interpretation, drafted and critically revised the manuscript; N. Koyama, Y. Isobe, Y. Ueda, Y. Kanai, E. Kondo, T. Fujii, M. Miura, contributed to conception and data acquisition, drafted and critically revised the manuscript; Kazuwa Nakao, K. Bessho, contributed to design and data acquisition, drafted and critically revised the manuscript. All authors gave final approval and agree to be accountable for all aspects of the work.

Acknowledgments

References

Arron JR, Winslow MM, Polleri A, Chang CP, Wu H, Gao X, Neilson JR, Chen L, Heit JJ, Kim SK, et al. 2006. NFAT dysregulation by increased dosage of DSCR1 and DYRK1A on chromosome 21. Nature. 441(7093):595–600.

Bagley CA, Pindrik JA, Bookland MJ, Camara-Quintana JQ, Carson BS. 2006. Cervicomedullary decompression for foramen magnum stenosis in achondroplasia. J Neurosurg. 104(Suppl 3):166–172.

Bellus GA, Hefferon TW, Ortiz de Luna RI, Hecht JT, Horton WA, Machado M, Kaitila I, McIntosh I, Francomano CA. 1995. Achondroplasia is defined by recurrent G380R mutations of FGFR3. Am J Hum Genet. 56(2):368–373.

Chusho H, Tamura N, Ogawa Y, Yasoda A, Suda M, Miyazawa T, Nakamura K, Nakao K, Kurihara T, Komatsu Y, et al. 2001. Dwarfism and early death in mice lacking C-type natriuretic peptide. Proc Natl Acad Sci USA. 98(7):4016–4021.

Cohen MM Jr. 1997. Short-limb skeletal dysplasias and craniosynostosis: what do they have in common? Pediatr Radiol. 27(5):442–446.

de Crombrugghe B, Lefebvre V, Nakashima K. 2001. Regulatory mechanisms in the pathways of cartilage and bone formation. Curr Opin Cell Biol. 13(6):721–728.

Di Rocco F, Dubravova D, Ziyadeh J, Sainte-Rose C, Collet C, Arnaud E. 2014. The foramen magnum in isolated and syndromic brachycephaly. Childs Nerv Syst. 30(1):165–172.

Elwood ET, Burstein FD, Graham L, Williams JK, Paschal M. 2003. Midface distraction to alleviate upper airway obstruction in achondroplastic dwarfs. Cleft Palate Craniofac J. 40(1):100–103.

Erdinçler P, Dashti R, Kaynar MY, Canbaz B, Ciplak N, Kuday C. 1997. Hydrocephalus and chronically increased intracranial pressure in achondroplasia. Childs Nerv Syst. 13(6):345–348.

Kake T, Kitamura H, Adachi Y, Yoshioka T, Watanabe T, Matsushita H, Fujii T, Kondo E, Tachibe T, Kawase Y, et al. 2009. Chronically elevated plasma C-type natriuretic peptide level stimulates skeletal growth in transgenic mice. Am J Physiol Endocrinol Metab. 297(6):E1339–E1348.

Lei WY, Wong RW, Rabie AB. 2008. Factors regulating endochondral ossification in the spheno-occipital synchondrosis. Angle Orthod. 78(2):215–220.

Lorget F, Kaci N, Peng J, Benoist-Lasselin C, Mugniery E, Oppeneer T, Wendt DJ, Bell SM, Bullens S, Bunting S, et al. 2012. Evaluation of the therapeutic potential of a CNP analog in a Fgfr3 mouse model recapitulating achondroplasia. Am J Hum Genet. 91(6):1108–1114.

Matsushita T, Wilcox WR, Chan YY, Kawanami A, Bukulmez H, Balmes G, Krejci P, Mekikian PB, Otani K, Yamaura I, et al. 2009. FGFR3 promotes synchondrosis closure and fusion of ossification centers through the MAPK pathway. Hum Mol Genet. 18(2):227–240.

Nakao K, Ogawa Y, Suga S, Imura H. 1992. Molecular biology and biochemistry of the natriuretic peptide system. II: Natriuretic peptide receptors. J Hypertens. 10(10):1111–1114.

Nakao K, Okubo Y, Yasoda A, Koyama N, Osawa K, Isobe Y, Kondo E, Fujii T, Miura M, Nakao K, et al. 2013. The effects of C-type natriuretic peptide on craniofacial skeletogenesis. J Dent Res. 92(1):58–64.

Nakao K, Osawa K, Yasoda A, Yamanaka S, Fujii T, Kondo E, Koyama N, Kanamoto N, Miura M, Kuwahara K, et al. 2015. The local CNP/GC-B system in growth plate is responsible for physiological endochondral bone growth. Sci Rep. 5:10554.

Nakao K, Yasoda A, Okubo Y, Yamanaka S, Koyama N, Osawa K, Isobe Y, Ikeno M, Fujii T, Kondo E. 2016. A novel therapeutic strategy for midfacial hypoplasia using the CNP/GC-B system. J Oral Maxillofac Surg Med Pathol. 29(1):10–16.

Naski MC, Colvin JS, Coffin JD, Ornitz DM. 1998. Repression of hedgehog signaling and BMP4 expression in growth plate cartilage by fibroblast growth factor receptor 3. Development. 125(24):4977–4988.

Richtsmeier JT, Baxter LL, Reeves RH. 2000. Parallels of craniofacial maldevelopment in Down syndrome and Ts65Dn mice. Dev Dyn. 217(2):137–145.

Shiang R, Thompson LM, Zhu Y-Z, Church DM, Fielder TJ, Bocian M, Winokur ST, Wasmuth JJ. 1994. Mutations in the transmembrane domain of FGFR3 cause the most common genetic form of dwarfism, achondroplasia. Cell. 78(2):335–342.

Suga S, Nakao K, Hosoda K, Mukoyama M, Ogawa Y, Shirakami G, Arai H, Saito Y, Kambayashi Y, Inouye K, et al. 1992. Receptor selectivity of natriuretic peptide family, atrial natriuretic peptide, brain natriuretic peptide, and C-type natriuretic peptide. Endocrinology. 130(1):229–239.

Takano T, Takigawa M, Shirai E, Nakagawa K, Sakuda M, Suzuki F. 1987. The effect of parathyroid hormone (1–34) on cyclic AMP level, ornithine decarboxylase activity, and glycosaminoglycan synthesis of chondrocytes from mandibular condylar cartilage, nasal septal cartilage, and spheno-occipital synchondrosis in culture. J Dent Res. 66(1):84–87.

Takigawa M, Okada M, Takano T, Ohmae H, Sakuda M, Suzuki F. 1984. Studies on chondrocytes from mandibular condylar cartilage, nasal septal cartilage, and spheno-occipital synchondrosis in culture. I. Morphology, growth, glycosaminoglycan synthesis, and responsiveness to bovine parathyroid hormone (1–34). J Dent Res. 63(1):19–22.

Tamura N, Doolittle LK, Hammer RE, Shelton JM, Richardson JA, Garbers DL. 2004. Critical roles of the guanylyl cyclase B receptor in endochondral ossification and development of female reproductive organs. Proc Natl Acad Sci USA. 101(49):17300–17305.

Thomas JN. 1978. Partial upper airway obstruction and sleep apnoea. J Laryngol Otol. 92(1):41–46.

Wealthall RJ, Herring SW. 2006. Endochondral ossification of the mouse nasal septum. Anat Rec A Discov Mol Cell Evol Biol. 288(11):1163–1172.

Yasoda A, Kitamura H, Fujii T, Kondo E, Murao N, Miura M, Kanamoto N, Komatsu Y, Arai H, Nakao K. 2009. Systemic administration of C-type natriuretic peptide as a novel therapeutic strategy for skeletal dysplasias. Endocrinology. 150(7):3138–3144.

Yasoda A, Komatsu Y, Chusho H, Miyazawa T, Ozasa A, Miura M, Kurihara T, Rogi T, Tanaka S, Suda M, et al. 2004. Overexpression of CNP in chondrocytes rescues achondroplasia through a MAPK-dependent pathway. Nat Med. 10(1):80–86.

Zhao X, Araki K, Miyazaki J, Yamamura K. 1992. Developmental and liver-specific expression directed by the serum amyloid P component promoter in transgenic mice. J Biochem. 111(6):736–738.